Electronic Supplementary Material (ESI) for Organic & Biomolecular Chemistry.

Electronic Supporting Information

Catching anions with coloured assemblies. Binding of pH-indicators by a giant-size polyammonium macrocycle for anion naked-eye recognition

Francesco Bartoli,[a] Andrea Bencini,[a] Luca Conti,[a] Claudia Giorgi,[a] Paola Paoli,[b] Patrizia Rossi,[b] Barbara Valtancoli,[a] Raphael Tripier[c]

Receptor and dye protonation

Considering that anion binding by polyamine macrocycle in aqueous solution depends on the number of protonated amine groups, the analysis of the basicity properties of receptor is a necessary requisite for the successive study of its interaction with anionic specie. Therefore, we preliminary determined the protonation constants of the receptor in $NaClO_4$ 0.1 M aqueous solution by means of As shown in Table S1, the ligand can bind up to ten H^+ ion in the pH range investigated (2.5-11.0). However, the first two protonation constants are too high to be determined in our experimental conditions and can be only estimated as higher than 11 log units. This behaviour can be related to the presence of cyclam moieties within the receptor structure. In fact, cyclam is known for its high value of its first protonation constant (log K = 11.29), due to the formation of a stabilizing network of hydrogen bonds involving the ammonium group and the adjacent amine function in the $(HCyclam)^+$ cation.[66] In the $(H_2L)^{2+}$ species the two ammonium group are reasonably located on two different cyclam units far one from each other. The two successive protonation steps present still high K_a values (ca 10 log. units). In the tetraprotonated receptor, the ammonium groups are reasonably located on four different cyclam moieties, thus minimizing the electrostatic repulsions. The successive protonation steps occur on cyclam macrocycles already containing an ammonium group. Interestingly enough, the constants for the equilibria $H^+ + (H_nL)^{n+} \rightleftharpoons (H_{n+1}L)^{(n+1)+}$ with n = 4-7 are similar to each other (they range from 8.72 and 8.0 log units), indicating that the corresponding protonation steps occur, once again, on four different cyclam moieties. Most likely, in the $(H_8L)^{8+}$ species each cyclam unit is diprotonated, the two acidic protons being localized on the secondary amine groups, more basic than tertiary ones in aqueous solution.[66,67] The remaining protonation steps necessarily occur on amine groups adjacent to two ammonium groups and induce a marked increase of the electrostatic repulsions between positive charges, thus accounting for the large drop of the basicity constant values observed passing from the eighth to the ninth protonation step. This scenario is reflected by the species distribution diagram depicted in Figure S1, which shows that the $(H_8L)^{8+}$ cation is the prevalent species in solution in a wide pH range, including neutral pH.

The protonation characteristics of four selected dyes have also been studied by coupling potentiometric, spectrophotometric and, in the case of fluorescein, fluorescence emission titrations in our experimental conditions. In all cases, the colour change occurs upon deprotonation of the phenolic –OH group. The relevant protonation equilibria and the corresponding pK_a values, determined by potentiometric titrations, are reported in Figure S2 and Table S2. The determined pK_a values are in good agreement with those reported in the literature.[67] Deprotonation of the

phenolic OH group generates in solution the dianionic species of the dyes and leads to marked changes in the absorption spectra and in the colours of dyes in solution (resumed in Figure S2). In most cases, deprotonation of the relevant phenolic –OH function induces the disappearance of the absorption band of the HD^- form of the dye (D = dye) and the simultaneous formation of a new absorption band at lower energy. This occurs in the case of bromocresol purple (herein indicated as H_2BCP in its neutral form) and phenol red (H_2PR), which feature two well distinct bands at 432 and 590 nm and 434 and 558 nm in their HD^- and D^{2-} forms, respectively. The pK_a values for the relevant $HD^- = D^{2-} + H^+$ equilibria, calculated in our experimental conditions by potentiometric titrations, result to be 6.3 and 7.7 for H_2BCP and H_2PR, respectively. In both cases, only a deprotonation equilibrium is detected in the pH range investigated (2-11), although in the case of H_2PR the formation at strongly acidic pH values (pK_a = 1.7) of a neutral species containing both phenol groups in their protonated form has been reported.[69] Conversely, in the case of fluorescein (H_2F) three deprotonation equilibria are found at acidic pH values, relative to the $H_3F^+ = H_2F + H^+$ (pK_a = 1.9), $H_2F = HF^- + H^+$ (pK_a = 4.0) and $HF^- = F^{2-} + H^+$ (pK_a = 6.7) equilibria, due to deprotonation of the carboxylic and two phenolic groups of the dye, respectively. The colour changes in this case are much less marked than in the case of H_2BCP and H_2PR, due to both the lower red shift of the absorption band occurring upon deprotonation of the phenol group and the yellow-green strong fluorescence emission, which makes the colour change less detectable by naked eye. The three forms of H_2F feature an absorption peak at 436 nm (H_3F^+ form), a broad band centered at 460 nm (H_2F and HF^-) and, finally, a band at 490 nm (F^{2-}). More interestingly, H_2F presents a marked pH-dependent fluorescence emission at 510 nm. In fact, the strong emission of F^{2-} is remarkably reduced in the HF^- form and the neutral form H_2F is basically not emissive.

As in the case of fluorescein, two successive deprotonation steps are also detected in the case of phenophtalein (H_2PP), with pK_a values of 8.6 (deprotonation of the carboxylic group) and 9.6 (deprotonation of the phenol function). The formation of the tricharged $PP(OH)^{3-}$ species, reported by some authors[67] at strongly alkaline pH values (pK_a ca 12) was not observed in our experimental conditions. Unlike the other dyes, the neutral H_2PP and the HPP^- forms do not feature absorption band in the visible region and H_2PP is basically colourless in aqueous solution below pH 9. Only the formation of the PP^{2-} form above pH 9 induces the formation of an absorption band at 552 nm, originating the well-known violet colour of the indicator. The spectra recorded at different pH values and a full list of the acid-base and spectroscopic characteristics of the indicators, determined in our experimental conditions, are given in Table S2 and Figures S2-S6).

Table S1. Protonation constants of receptor L in $NaClO_4$ 0.1 M at 298 K.

Equilibrium	**log K**
$H^+ + (H_2L)^{2+} \rightleftharpoons (H_3L)^{3+}$	10.06(7)
$H^+ + (H_3L)^{3+} \rightleftharpoons (H_4L)^{4+}$	9.90(7)
$H^+ + (H_4L)^{4+} \rightleftharpoons (H_5L)^{5+}$	8.72 (6)
$H^+ + (H_5L)^{5+} \rightleftharpoons (H_6L)^{6+}$	8.54(7)
$H^+ + (H_6L)^{6+} \rightleftharpoons (H_7L)^{7+}$	8.1 (1)
$H^+ + (H_7L)^{7+} \rightleftharpoons (H_8L)^{8+}$	8.0 (1)
$H^+ + (H_8L)^{8+} \rightleftharpoons (H_9L)^{9+}$	4.6 (1)
$H^+ + (H_9L)^{9+} \rightleftharpoons (H_{10}L)^{10+}$	2.2 (1)

Table S2. pK_a values and main photophysical characteristics of bromocresol purple (H_2BCP), phenol red (H_2PR), phenopthalein (H_2PP) and fluorescein (H_2F) in our experimental conditions.

Indicator	**Species in aqueous solution**	**Colour and molar extinction coefficient in water (dm^3mol^{-1} cm^{-1})**	**pK_a**
Bromocresol purple (H_2BCP)	$HBCP^-$	Yellow, 17610 (λ = 432 nm)	6.3(1)
	BCP^{2-}	Violet, 40475 (λ = 590 nm)	
Phenol red (H_2PR)	HPR^-	Yellow, 27084 (λ = 434 nm)	7.7(1)
	PR^{2-}	Red, 69441 (λ = 558 nm)	
Phenopthalein (H_2PP)	H_2PP	Colorless	8.6(1)
	HPP^-	Colorless	9.6(1)
	PP^{2-}	Violet, 9667 (λ = 552 nm)	
fluorescein (H_2F)	H_3F^+	Yellow, 35312 (λ = 436 nm), not emissive	1.9(1)
	H_2F	Yellow, 18192 (λ = 460 nm), not emissive	4.0(1)
	HF^-	Yellow, 29109 (λ = 460 nm) weakly emissive at 510 nm	6.7(1)
	F^{2-}	Intense yellow,78210 (λ = 490 nm) emissive at 510 nm	

Table S3. Stability constants of the adducts formed by fluorescein with L ($NaClO_4$ 0.1 M aqueous solution, 298 K).

Reaction	logK
$F^{2-} + (H_2L)^{2+} \rightleftharpoons [H_2LF]$	4.2(5)
$F^{2-} + (H_3L)^{3+} \rightleftharpoons [H_3LF]^{+}$	4.4(3)
$F^{2-} + (H_4L)^{4+} \rightleftharpoons [H_4LF]^{2+}$	5.4(2)
$F^{2-} + (H_5L)^{5+} \rightleftharpoons [H_5LF]^{3+}$	5.8(1)
$F^{2-} + (H_6L)^{6+} \rightleftharpoons [H_6LF]^{4+}$	6.8(1)
$F^{2-} + (H_7L)^{7+} \rightleftharpoons [H_7LF]^{5+}$	7.5(2)
$F^{2-} + (H_8L)^{8+} \rightleftharpoons [H_8LF]^{6+}$	7.7(1)
$HF^{-} + (H_8L)^{8+} \rightleftharpoons [H_9LF]^{7+}$	4.4(1)
$HF^{-} + (H_9L)^{9+} \rightleftharpoons [H_{10}LF]^{8+}$	5.0(1)
$2F^{2-} + (H_2L)^{2+} \rightleftharpoons [H_2LF_2]^{2-}$	8.0(1)
$2F^{2-} + (H_4L)^{4+} \rightleftharpoons [H_4LF_2]$	10.2(1)
$2F^{2-} + (H_6L)^{6+} \rightleftharpoons [H_6LF_2]^{2+}$	13.1(1)
$2F^{2-} + (H_8L)^{8+} \rightleftharpoons [H_8LF_2]^{4+}$	15.2(1)

Table S4. Stability constants of the adducts formed by phenol red with L ($NaClO_4$ 0.1 M aqueous solution, 298 K).

Reaction	logK
$PR^{2-} + (H_2L)^{2+} \rightleftharpoons [H_2LPR]$	5.9(5)
$PR^{2-} + (H_3L)^{3+} \rightleftharpoons [H_3LPR]^{+}$	6.5(3)
$PR^{2-} + (H_4L)^{4+} \rightleftharpoons [H_4LPR]^{2+}$	7.0(2)
$PR^{2-} + (H_5L)^{5+} \rightleftharpoons [H_5LPR]^{3+}$	7.9(1)
$PR^{2-} + (H_6L)^{6+} \rightleftharpoons [H_6LPR]^{4+}$	8.2(1)
$PR^{2-} + (H_7L)^{7+} \rightleftharpoons [H_7LPR]^{5+}$	8.7(2)
$PR^{2-} + (H_8L)^{8+} \rightleftharpoons [H_8LPR]^{6+}$	9.3(1)
$HPR^{-} + (H_8L)^{8+} \rightleftharpoons [H_9LPR]^{7+}$	9.8(1)
$HPR^{-} + (H_9L)^{9+} \rightleftharpoons [H_{10}LPR]^{8+}$	6.1(1)
$2PR^{2-} + (H_2L)^{2+} \rightleftharpoons [H_2LPR_2]^{2-}$	11.5(1)
$2PR^{2-} + (H_4L)^{4+} \rightleftharpoons [H_4LPR_2]$	13.4(1)
$2PR^{2-} + (H_6L)^{6+} \rightleftharpoons [H_6LPR_2]^{2+}$	16.1(1)
$2PR^{2-} + (H_8L)^{8+} \rightleftharpoons [H_8LPR_2]^{4+}$	18.0(1)

Table S5. Stability constants of the adducts formed by phenopthalein with L ($NaClO_4$ 0.1 M aqueous solution, 298 K).

Reaction	logK
$PP^{2-} + (H_2L)^{2+} \rightleftharpoons [H_2LPP]$	5.8(1)
$PP^{2-} + (H_3L)^{3+} \rightleftharpoons [H_3LPP]^{+}$	6.0(3)
$PP^{2-} + (H_4L)^{4+} \rightleftharpoons [H_4LPP]^{2+}$	6.6(2)
$HPP^{-} + (H_4L)^{4+} \rightleftharpoons [H_5LPP]^{3+}$	4.9(1)
$2PP^{2-} + (H_2L)^{2+} \rightleftharpoons [H_2LPP_2]^{2-}$	10.8(1)
$2PP^{2-} + (H_4L)^{4+} \rightleftharpoons [H_4LPP_2]$	12.4(1)

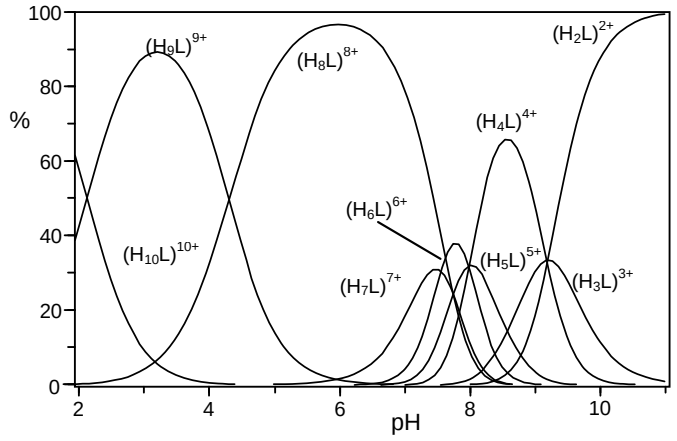

Fig. S1. Distribution diagrams of the protonated forms of L ($NaClO_4$ 0.1 M aqueous solution, 298 K).

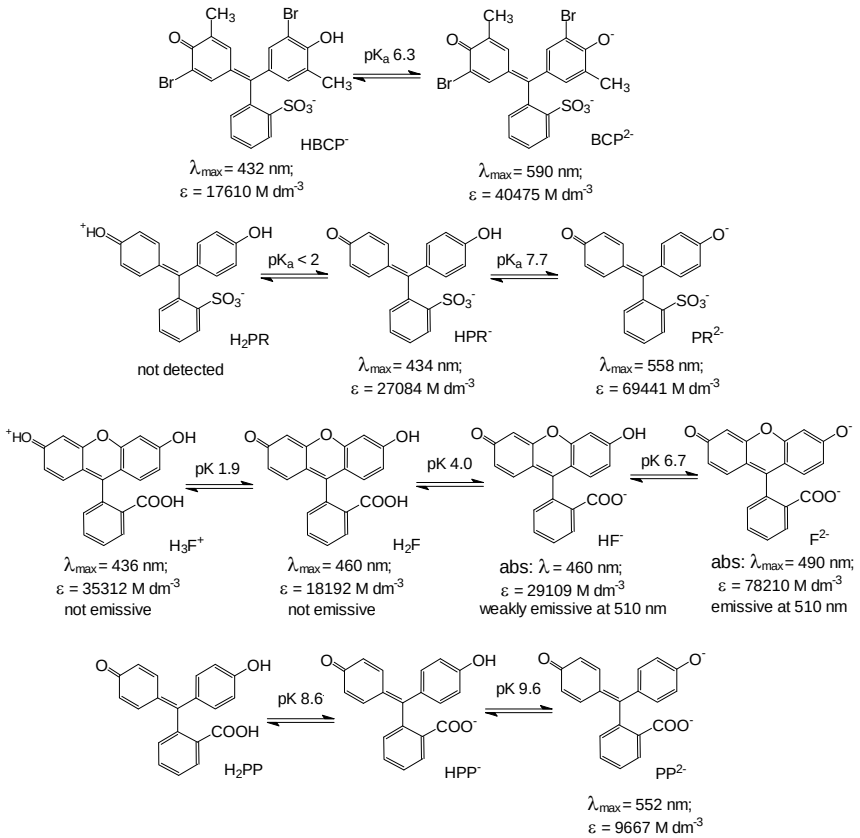

Figure S2. Protonation equilibria in the four indicators and corresponding pK_a value.

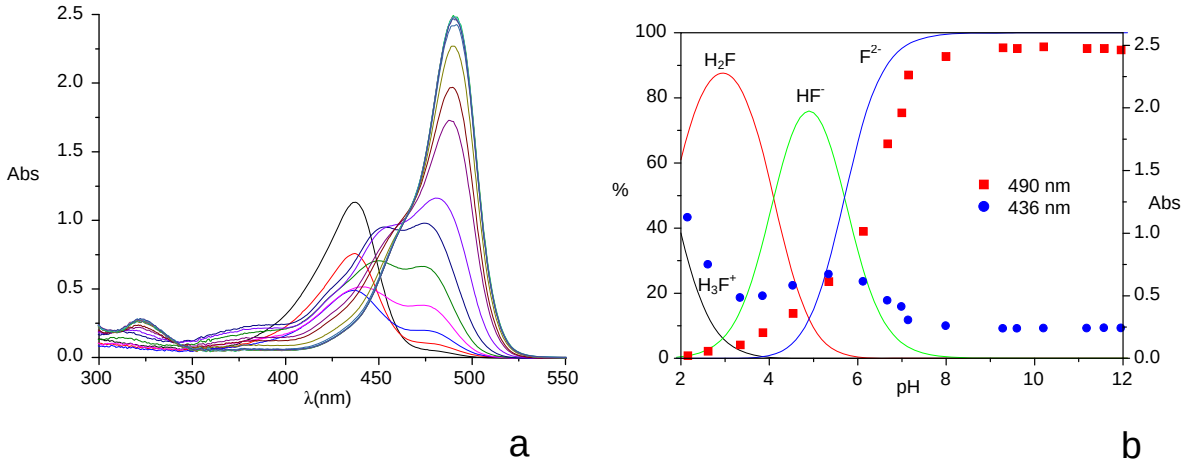

Figure S3. UV-visible absorption spectra of fluorescein in water at different pH values (a), and absorption values of fluorescein at 490 (■) and 436 (●) nm compared to the distribution diagrams of the protonated species of fluorescein (b). $[H_2F]= 3.2 \times 10^{-5}$ M.

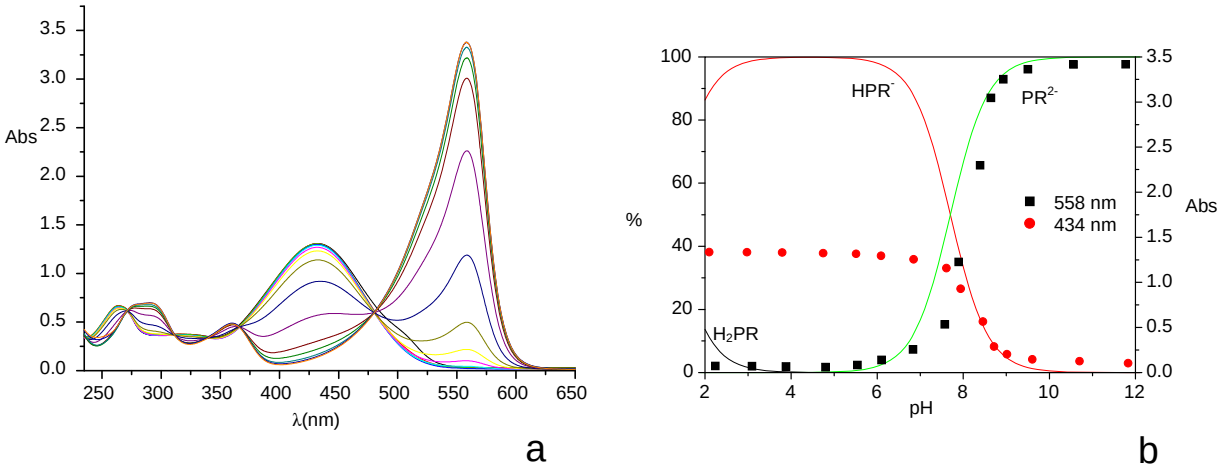

Figure S4. UV-visible absorption spectra of phenol red in water at different pH values (a), and absorption values of phenol red at 558 (■) and 434 (●) nm compared to the distribution diagrams of the protonated species of phenol red (b). $[H_2PR]= 4.97 \times 10^{-5}$ M.

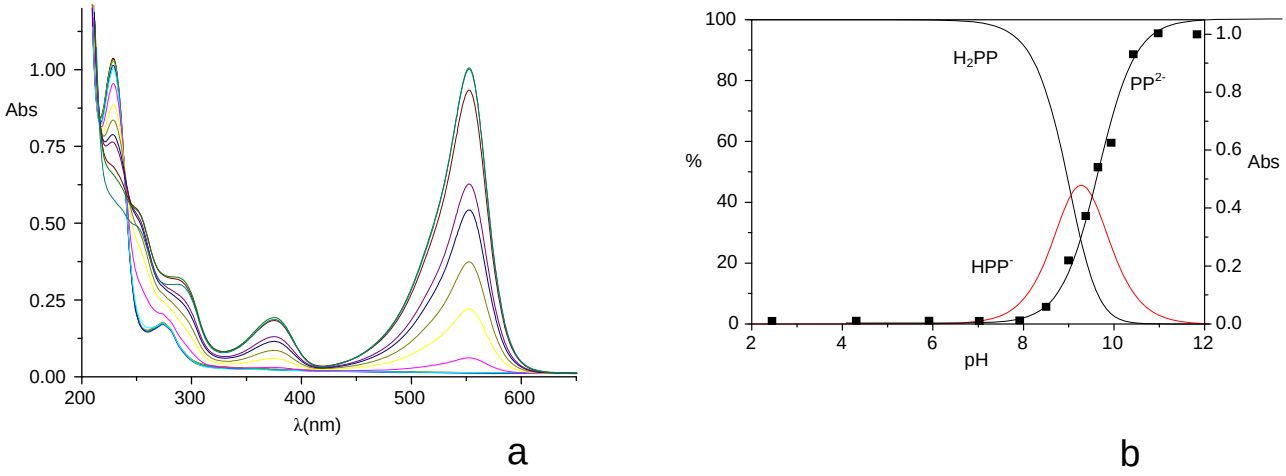

Figure S5. UV-visible absorption spectra of phenopthalein in water at different pH values (a), and absorption values of phenopthalein at 552 nm (■) compared to the distribution diagrams of the protonated species of phenopthalein (b). [H_2PP]= 1.04 x 10^{-4} M.

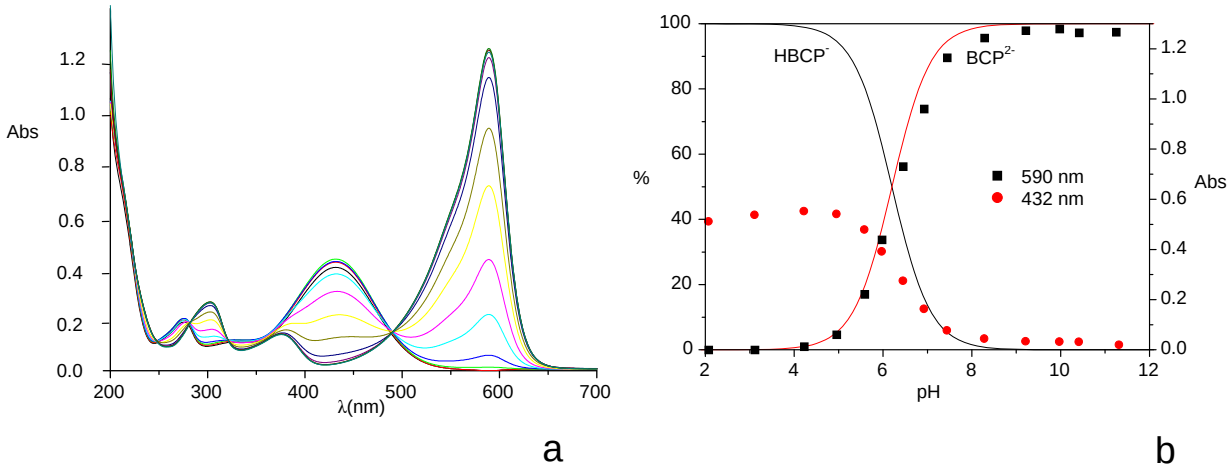

Figure S6. UV-visible absorption spectra of bromocresol purple in water at different pH values (a), and absorption values of bromocresol purple at 590 (■) and 432 (●) nm compared to the distribution diagrams of the protonated species of bromocresol purple (b). [H_2BCP]= 3.15 x 10^{-5} M.

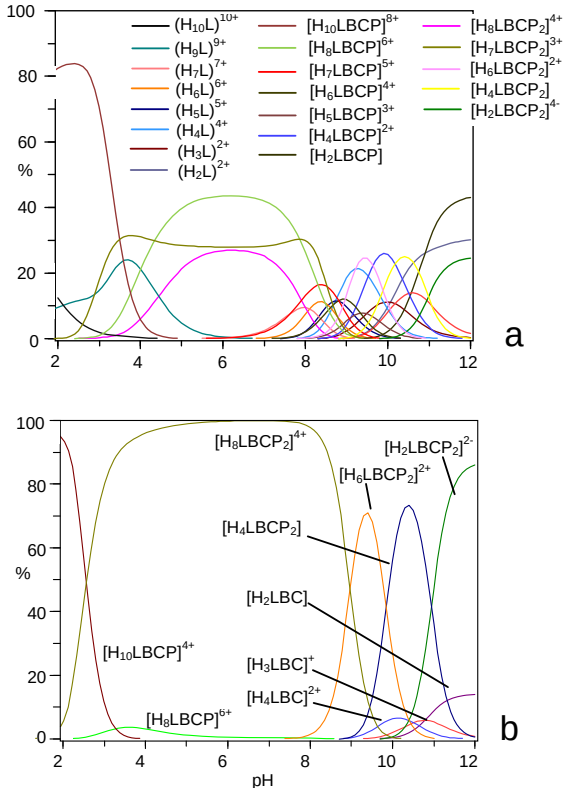

Figure S7. Distribution diagrams of the adducts formed by L in the presence of 1 equiv. (a) or two equivs. (b) of H_2BCP ([L] = $1 \cdot 10^{-4}$ M).

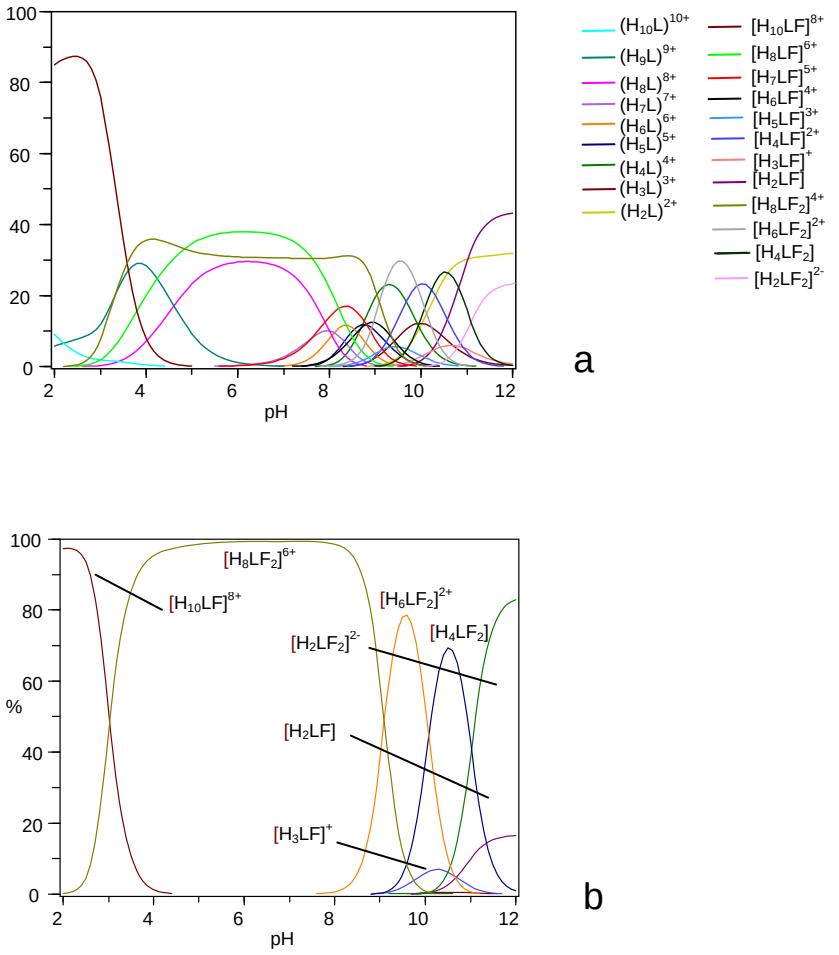

Figure S8. Distribution diagrams of the adducts formed by L in the presence of 1 equiv. (a) or two equivs. (b) of H_2F. ([L] = 1 x 10^{-3} M).

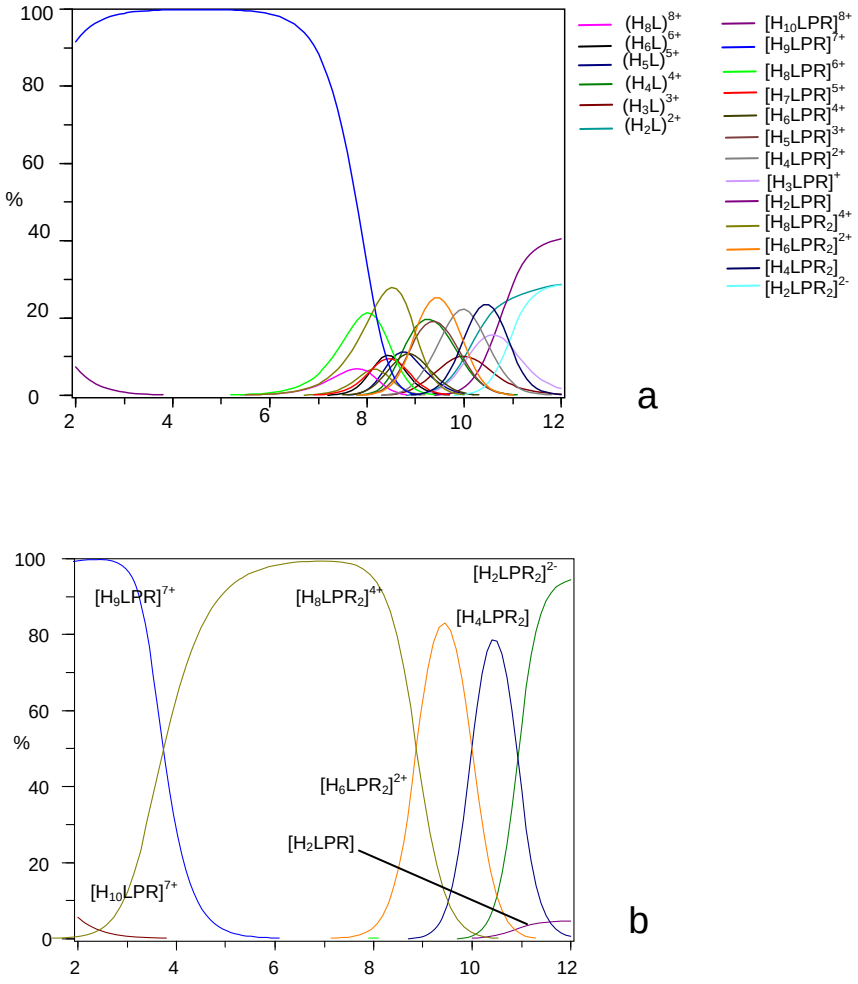

Figure S9. Distribution diagrams of the adducts formed by L in the presence of 1 equiv. (a) or two equivs. (b) of H_2PR. ([L] = 1 x 10^{-3} M).

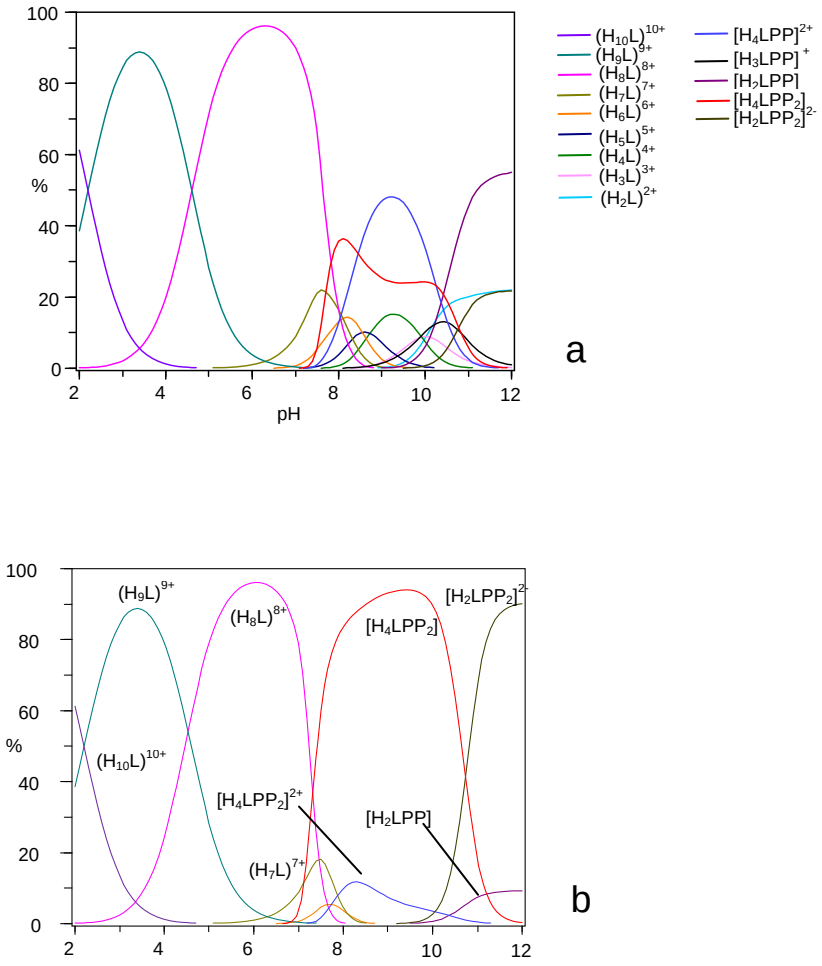

Figure S10. Distribution diagrams of the adducts formed by L in the presence of 1 equiv. (a) or two equivs. (b) of H_2PP. ([L] = 1 x 10^{-3} M).

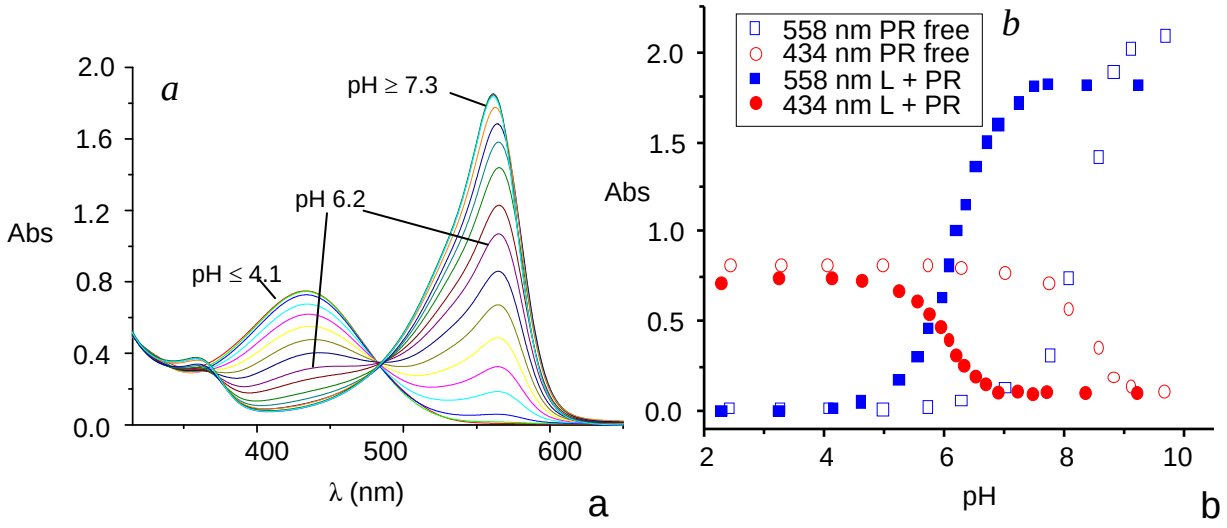

Figure S11. UV visible spectra of H_2PR in the presence of L at different pH values (a) and absorbance measured at 434 (circle) and 558 (square) nm in the absence (empty symbols) and in the presence (filled symbols) of 0.5 equivs. of L ([H_2PR] = 3.0 x 10^{-5} M).

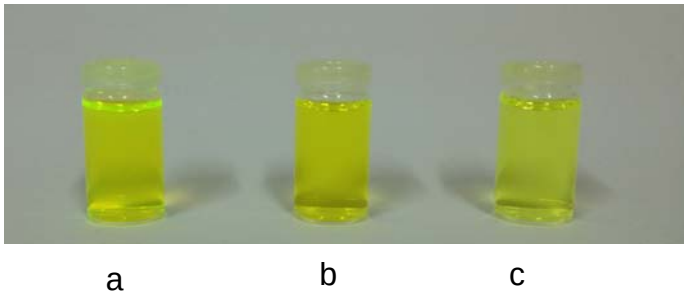

Figure S12. Photographs of solutions of H_2F in the presence of the L (0.5 equivs) at pH 1.9, (a), 5.4 (b) and 8.5 (c) ([H_2F] = 3.2 x 10^{-5} M)

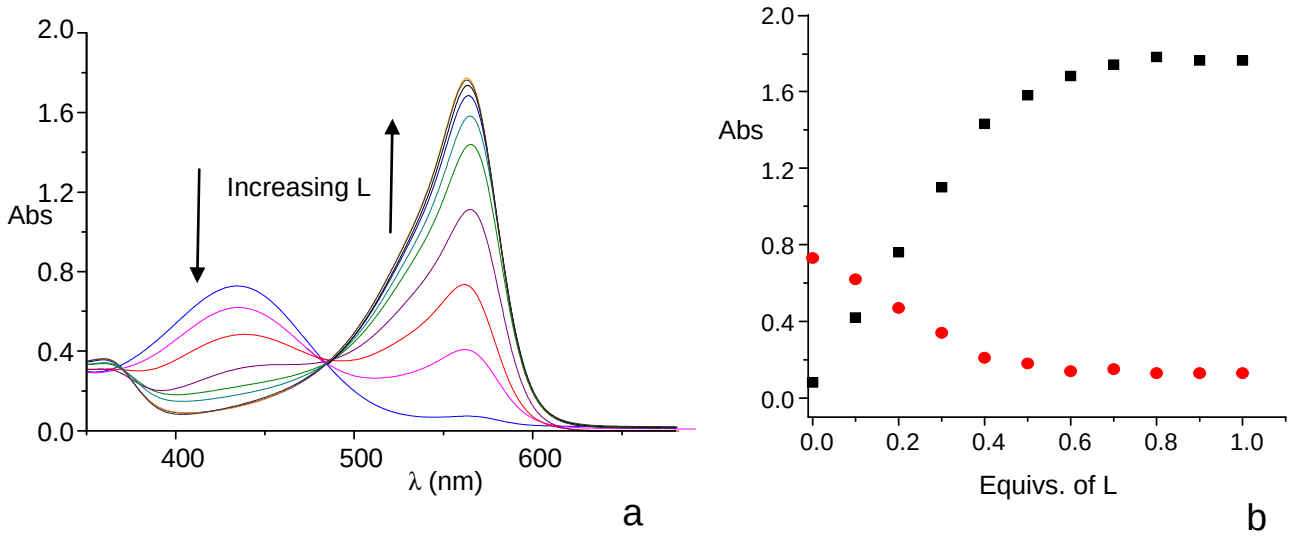

Figure S13. UV visible spectra (a) and absorbance values at 558 nm (■) and 434 nm (●) (b) of H_2PR at pH 7 in the presence of increasing amount of L ([H_2PR]= 2.9 x 10^{-5} M).

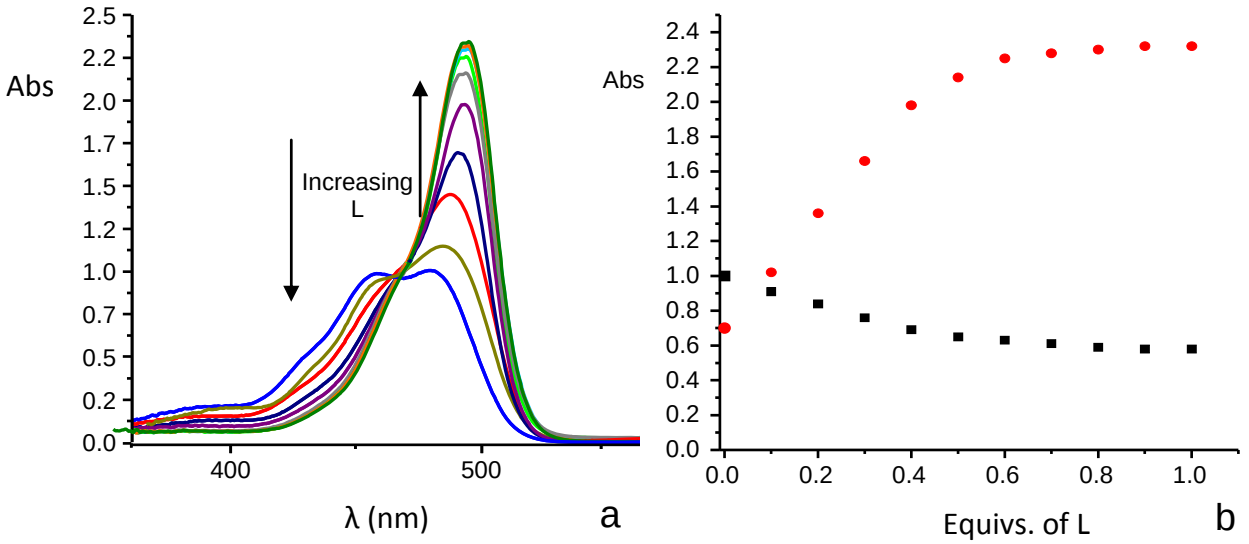

Figure S14. UV visible spectra (a) and absorbance values at 450 nm (■) and 490 nm (●) (b) of H_2F at pH 5.4 in the presence of increasing amount of L ([H_2F] = 3.2 x 10^{-5} M).

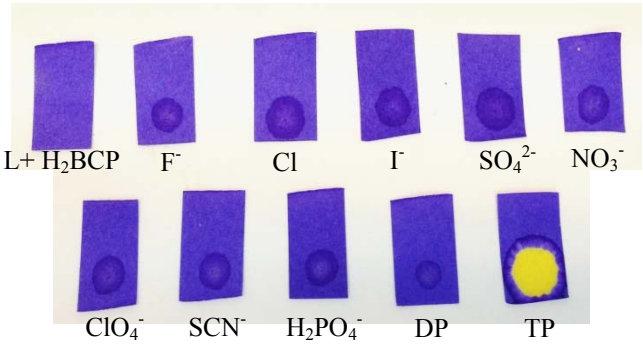

Figura S15. Photographs of stripes of filter paper soaked with a solution of L/H_2BCP ensemble after the addition of a drop of a solution at pH 5.4 of the different anions.

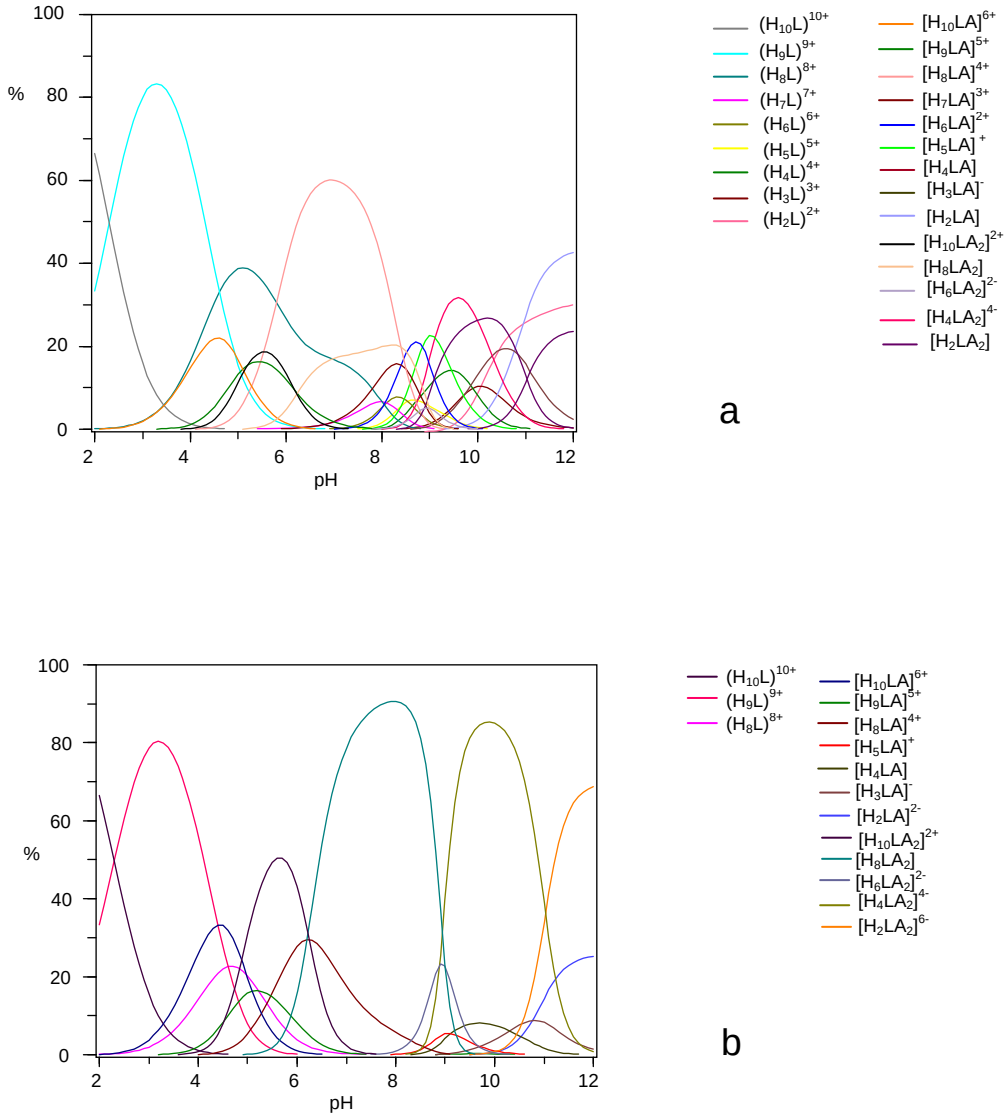

Figure S16. Distribution diagrams of the adducts formed by L in the presence of 1 equiv. (a) or two equivs. (b) of diphosphate (A = $P_2O_7^{4-}$). ([L] = 1 x 10^{-3} M]).

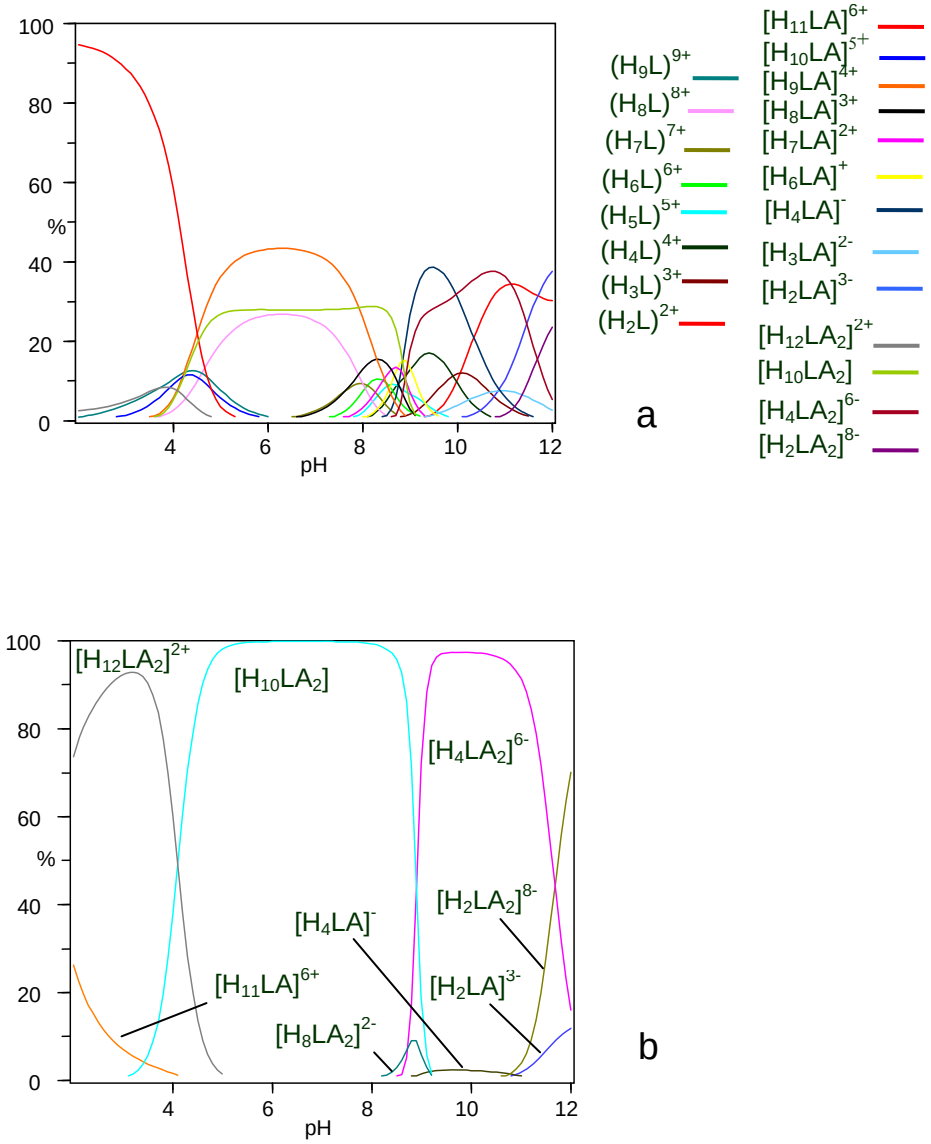

Figure S17. Distribution diagrams of the adducts formed by the L in the presence of 1 equiv. (a) or two equivs. (b) of triphosphate (A = $P_3O_{19}^{5-}$).). ([L] = 1 x 10^{-4} M]).